Ordered nanoporous polymer–carbon composites

MINKEE CHOI AND RYONG RYOO*

National Creative Research Initiative Center for Functional Nanomaterials, and Department of Chemistry (School of Molecular Science-BK21), Korea Advanced Institute of Science and Technology, Daejeon, 305-701, Korea

*e-mail: rryoo@kaist.ac.kr

Published online: 22 June 2003; doi:10.1038/nmat923

Nanostructured organic materials, particularly those constructed with uniform nanopores, have been sought for a long time in materials science[1–7]. There have been many successful reports on the synthesis of nanostructured organic materials using the so-called, 'supramolecular liquid crystal templating' route[8–13]. Ordered nanoporous polymeric materials can also be synthesized through a polymerization route using colloidal[14,15] or mesoporous silica[16,17] templates. The organic pore structures constructed by these approaches, however, are lower in mechanical strength and resistance to chemical treatments than nanoporous inorganic, silica and carbon materials. Moreover, the synthesis of the organic materials is yet of limited success in the variation of pore sizes and structures, whereas a rich variety of hexagonal and cubic structures is available with tunable pore diameters in the case of the inorganic materials[18–20]. Here we describe a synthesis strategy towards ordered nanoporous organic polymers, using mesoporous carbon as the retaining framework. The polymer–carbon composite nanoporous materials exhibit the same chemical properties of the organic polymers, whereas the stability of the pores against mechanical compression, thermal and chemical treatments is greatly enhanced. The synthesis strategy can be extended to various compositions of hydrophilic and hydrophobic organic polymers, with various pore diameters, connectivity and shapes. The resultant materials exhibiting surface properties of the polymers, as well as the electric conductivity of the carbon framework, could provide new possibilities for advanced applications. Furthermore, the synthesis strategy can be extended to other inorganic supports such as mesoporous silicas.

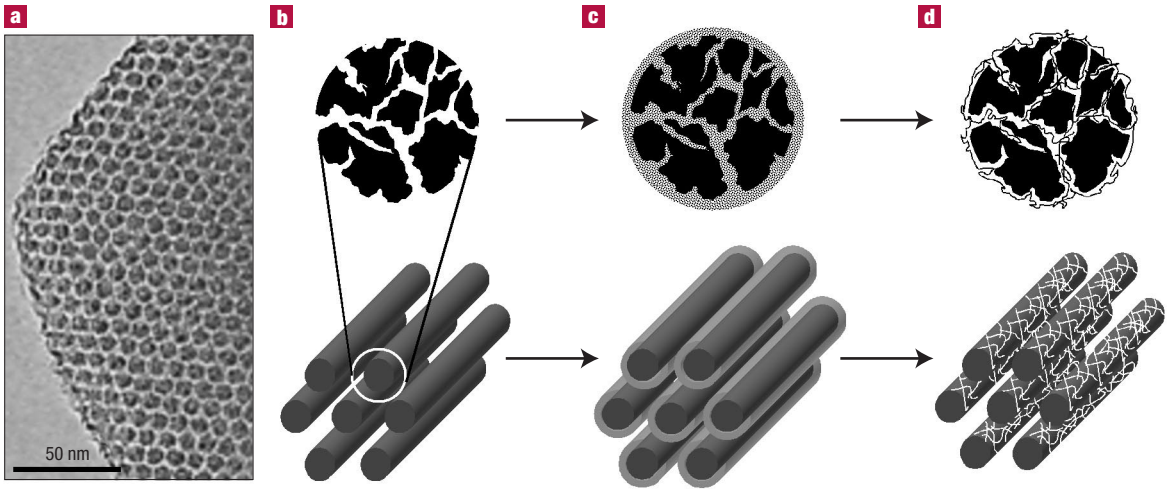

Figure 1 The synthesis route to nanoporous polymer–carbon composite materials. a, Transmission electron microscope image of the CMK-3 mesoporous carbon, showing the hexagonal array of carbon nanorods. These rods are rigidly interconnected with uniform spacing using carbon spacers, which are random in thickness and location along the direction of the nanorods. **b**, Structural model of the carbon nanorods with microporosity (carbon spacers are omitted). **c**, The impregnation of organic monomers into CMK-3 carbon. The monomer loading is controlled so that the monomers should fill micropores and form a thin film on the nanorod surface, without causing capillary condensation in the mesopores between nanorods. **d**, Polymerization of monomers into crosslinked polymers. The resultant polymers form interpenetrating, inseparable composite frameworks with carbon.

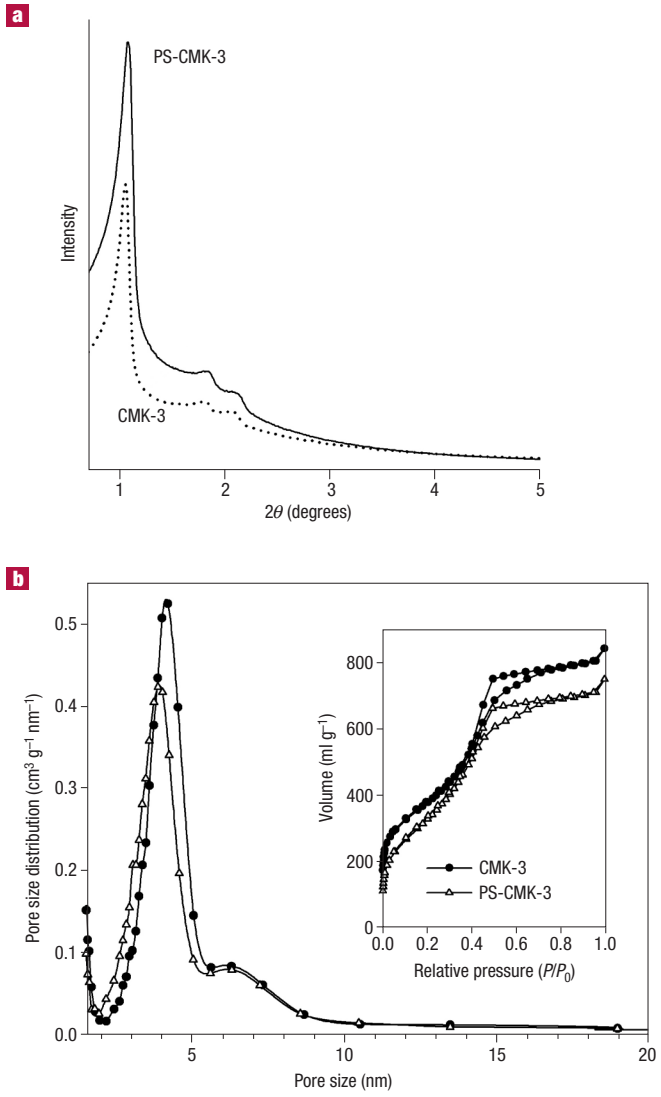

Figure 2 X-ray powder diffraction (XRD) patterns and pore-size distributions for CMK-3 mesoporous carbon and its composite material with crosslinked polystyrene (PS-CMK-3, 45 wt% polymer-loading on carbon). a, The XRD intensity of the polymer–carbon composite is significantly increased from that of the original carbon, due to the polymer filling in micropores of the carbon frameworks. **b**, The pore-size distribution of CMK-3 and PS-CMK-3 determined by Barrett-Joyner-Halenda (BJH) analysis of the N_2 adsorption isotherm (inset). The mesopore diameters changed from 4.2 to 3.9 nm with the polymer loading. P = N_2 pressure in contact with the sample; P_0 = vapour pressure of liquid N_2 at 77 K.

The present synthesis strategy is to impregnate ordered mesoporous (or nanoporous) carbon materials[21–25] that are highly microporous in the mesopore walls (or frameworks) with organic monomers. The impregnation is controlled so that the micropores are completely filled with organic monomers, and also that the mesopore walls are coated with a thin layer of monomers. The monomers are subsequently converted to crosslinked polymers. The organic nanopores thus constructed exhibit highly enhanced stability, due to the formation of interpenetrating composite frameworks between the crosslinked polymers and carbon (see Fig. 1).

The ordered mesoporous carbons suitable for this purpose are available with various pore arrangements (hexagonal and cubic structures) and diameters (typically, ranging from 2 to 10 nm), through the synthesis route using mesoporous silica templates[21–25]. The structure of the mesoporous carbons is characterized by the three-dimensional interconnection of nanorods or nanobeads, which seem to be uniform in diameter, typically in the range of several nanometres. The regular nanoscale spacings between the nanoframeworks impart these materials, referred to as CMK, with uniform mesoporosity. The carbon frameworks can be fabricated with high microporosity as illustrated in Fig. 1. These micropores are the preferred adsorption sites for mesopores for many organic adsorbates. Organic adsorbates start filling the mesopores by capillary condensation after the micropores in the mesopore walls have been completely filled, and the wall surface is coated with a thin film of adsorbates. Based on these adsorption phenomena, we have designed the synthesis procedure for a crosslinked polystyrene(PS)-CMK-3 composite (see Methods). We have confirmed that this procedure can be generalized for various hydrophilic and hydrophobic organic polymers, such as crosslinked poly(methyl methacrylic acid) and poly(2-hydroxyethyl methylmethacrylate), whereas the CMK carbons have high affinity with a wide variety of monomers of different hydrophobic nature. The polymer content can be increased to as much as 45 wt% of carbon without causing mesopore blockage. Our synthesis results have been confirmed by gravimetric analysis of the sample weight, pore-size distribution measurement, and most evidently, X-ray powder diffraction (XRD) intensity.

Generally, the XRD pattern for ordered mesoporous materials is composed of distinct diffraction lines appearing at low angles (typically, where $2\theta < 5°$), which are used for the determination of the structure. These XRD lines decrease in intensity as guest species are loaded in the mesopores, and such an intensity change is a useful means of judging the location of the guest species. However, contrary to most cases, our CMK carbons exhibit a significant increase in the diffraction intensity when organic polymers are synthesized within the structure following the procedure described in the Methods section. The XRD result for the PS in CMK-3 carbon is shown in Fig. 2a. The XRD data indicate that the polymerization inside micropores results in an increase of the apparent density of the mesopore walls. This distinctive phenomenon is similar to the intensity increase in the neutron-diffraction when N_2 is preferentially adsorbed, at low pressure, inside micropores that are present in the mesopore walls of some mesoporous silicas[26,27]. The mesopore vacancy in the carbon–polymer composite has been confirmed by pore-size analysis using the Barrett–Joyner–Halenda (BJH) algorithm (Fig. 2b). For example, the CMK-3 carbon indicates only a small decrease from 4.2 to 3.9 nm in the median mesopore diameter, even when the PS loading is increased up to 45 wt% of carbon. We have measured the mesopore volume corresponding to the capillary condensation around $P/P_0 = 0.4$ (see inset of Fig. 2b). This experiment revealed that the polymer loading caused the mesopore volume corresponding to 2–10 nm pores to decrease by only 7% (based on the same carbon weight), despite the 45 wt% polymer-loading.

Despite the highly porous architecture, the CMK carbons exhibit high mechanical stability under compression. Interestingly, the mechanical stability increases further with the incorporation of polymers (see Supplementary Information), showing a synergistic enhancement between the carbon framework and the polymer. The PS-CMK-3 composite material maintained the highly ordered nanostructure after being pressed for 10 min at 1,500 MPa. In addition, the structure was maintained after heating at 150 °C, or washed with chloroform, as shown by the same XRD pattern and N_2 adsorption isotherm as those for the pristine sample. The high stability is a remarkable advantage in that it permits safe chemical functionalization under harsh conditions, such as heating in strong acids and solvents. For example, the polymer in the PS-CMK-3 system could be sulphonated using concentrated sulphuric acid at 100 °C (1.0 g of the

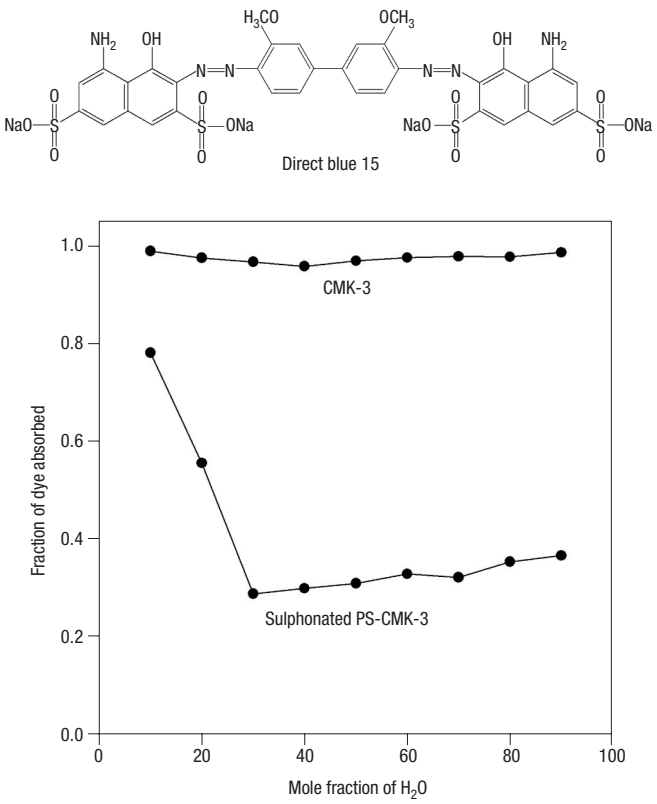

Figure 3 Elution of 'Direct Blue 15' (an organic dye with 3.3 nm rod-like molecular geometry) after adsorption on CMK-3 and sulphonated PS-CMK-3 composite. The adsorption was performed from a dye solution prepared by using ethanol–water mixture as a solvent (1×10^{-4} M, 0.1 ml), at the top of a column of 0.7 cm diameter, and packed with 0.3 g sample. The adsorbed dye was eluted by flow of the ethanol–water mixture at the rate of 0.1 ml min^{-1}. The dye concentration in the first 2 ml eluent was analysed by the light absorption at 600 nm wavelength (JASCO V-530 ultraviolet/visible spectrophotometer).

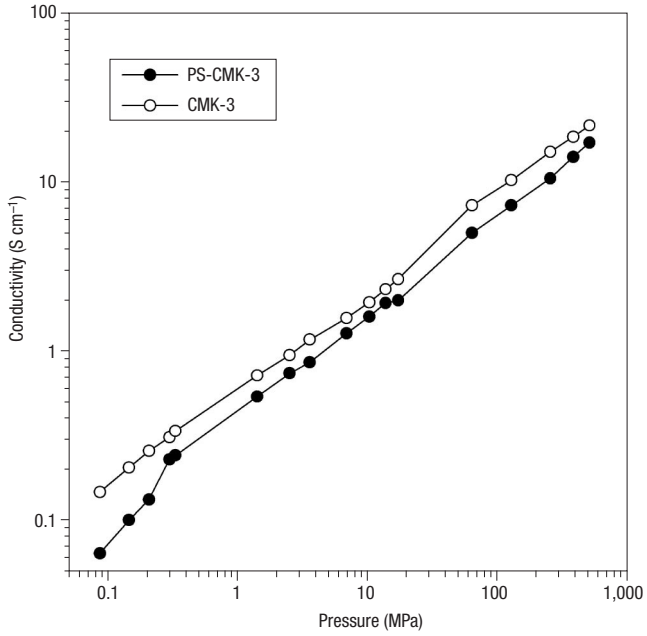

Figure 4 The electric conductivities of CMK-3 mesoporous carbon and PS-CMK-3, plotted as a function of compressive pressure at room temperature. The conductivities were measured with a home-built apparatus following the four-point probe method[30]. The conductivity of CMK-3 does not decrease significantly, even after loading of 45 wt% polystyrene.

composite was stirred for 4 h at 100 °C in 20 ml 98% sulphuric acid). The resulting product exhibited the specific BET surface area of 650 m^2 g^{-1}, and about the same pore-size distribution as the material before the sulphonation. Titration with NaOH revealed that the sulphonated PS-CMK-3 contained acid groups amounting to 3.5×10^{-3} mol g^{-1} polymer (after subtraction of 10.3% of the total value for the acid density of CMK-3 treated under the same condition). This result is very remarkable for a PS containing as much as 20 mol% divinylbenzene (DVB), whereas the ion-exchange capacity of ordinary commercial crosslinked PS resins ranges from 1.8–4.8×10^{-3} mol g^{-1}, and decreases rapidly as the DVB content exceeds the commercial range of 2–8 mol%.

The PS-CMK-3 nanoporous material has quite a distinct surface nature, compared with the mesoporous carbon. As shown in Fig. 3, a column packed with sulphonated PS-CMK-3 gave different eluate concentrations depending on the solvent composition. In the case of CMK-3 carbon, the dye was so strongly adsorbed that it was difficult to remove from the column at any solvent composition. The dye adsorption data indicate that the nanopore walls are effectively coated with a thin layer of polymer. Interestingly, such a thin layer of polymer does not cause a significant decrease in the electric conductivity. This has been confirmed by the comparison of the electric conductivity between PS-CMK-3 (unsulphonated) and CMK-3 (Fig. 4). These properties may offer a remarkable advantage for applications to functional electrode materials such as amperometric biosensors[28,29]. The ion-exchanging polymer–carbon composite may also provide unique opportunities for the design of fuel-cell electrode materials that can support high dispersions of platinum nanoparticles[24] and possess high ionic conductivity simultaneously.

The present strategy to support organic polymers on carbon frameworks may be extended to other nanoporous materials such as mesoporous silicas and colloidal crystals, as long as the supported polymer layer can be anchored to the nanopore walls. For example, the SBA-15 mesoporous silica can be synthesized with highly microporous frameworks. We have confirmed that various polymers, such as crosslinked poly(2-hydroxyethyl methacrylate) and poly(methyl methacrylate) can be supported onto such SBA-15 silicas (M. Choi and R. Ryoo, manuscript in preparation). The resultant polymer–silica composite materials possess uniform mesoporosity, and the XRD intensity increases, similar to the aforementioned case of PS-CMK. In addition, the composite materials exhibit significantly enhanced hydrothermal stability in boiling water. However, it is noteworthy that microporosity of the mesoporous silica walls varies widely depending on the details of the synthesis conditions. In the case of silica pore walls with low microporosity, we have failed to form a film of polymers without causing pore blockage.

In conclusion, we propose that the present strategy should provide a versatile route to nanoporous polymer–carbon composites with various compositions and pore architectures. The polymer–carbon composite materials can be obtained with uniform porosity, various pore sizes (typically, in the range 2–10 nm), shapes and connectivity, taking advantage of the structural variation of the carbon supports. High thermal and chemical stabilities of the polymer-like pore walls supported on the carbon frameworks is an advantage for functionalization. The polymer–carbon composite can have the surface

nature of polymers while the electric conductivity of the original carbon is maintained, which suggests new application possibilities as advanced electrode materials. Furthermore, the present synthesis strategy can be extended from carbon to porous silica materials. Owing to their properties such as high surface area, regular pore structure, high capacity for metal dispersion and facile chemical functionalizability, we believe that the nanoporous composite system could find broad applications in many areas of materials science, including separation of biomaterials, removal of pollutants, selective ion exchange, and manufacturing of high-performance catalysts and sensors.

METHODS

MATERIALS SYNTHESIS

The ordered mesoporous carbon referred to as CMK-3 was synthesized by pyrolysis of sucrose inside the SBA-15 mesoporous silica, following the procedure reported elsewhere[25]. The silica template was subsequently removed by washing with HF solution twice, and evacuated for the removal of moisture at 300 °C. Divinylbenzene (DVB, Aldrich, 80%) and styrene (Janssen, 99%) were purified through an alumina column to remove polymerization inhibitors. 1 g CMK-3 was impregnated with a mixture of 0.356 g DVB/0.112 g styrene/0.026 g 2,2′-azobisisobutyronitrile/1.09 g methylene chloride. After the methylene chloride was evaporated in a drying oven for 3 h at 60 °C, the CMK-3 sample containing the organic monomers and the polymerization initiator was sealed under argon atmosphere. The sample was subsequently heated as sealed for two days at 150 °C for polymerization. The sample was thoroughly washed with chloroform and dried in a vacuum oven. The polymer content in the organic-carbon composite thus obtained was analysed from the increase in sample weight due to the organic incorporation. This analysis revealed that the sample weight increased by 45 wt% of the carbon weight, which indicates that over 90% of the organic monomers were polymerized to form an inseparable composite with carbon frameworks.

It should be noted that the use of methylene chloride and its subsequent evaporation was an effective way to achieve polymerization in the desired locations. The solvent was useful to achieve uniform distribution of the small amount of monomers and initiator that amounted to only 40% of the pore volume. When the solvent was not removed, the polymerization resulted in mesopore blockage. The XRD intensity decreased as a result of the polymer location in the mesopores, and no dye adsorption occurred at any solvent compositions between water and ethanol due to mesopore blockage.

MEASUREMENTS

XRD patterns were recorded by using a Rigaku multiflex diffractometer equipped with CuKα radiation (40 kV, 50 mA). XRD scanning was performed under ambient conditions over the 2θ region 0.7–5° at steps of 0.01° and accumulation time 5 s per step. TEM images were obained with a JEOL JEM-4000EX operated at 400 kV. Samples for TEM measurements were suspended in ethanol and supported on a carbon-coated copper grid. N_2 adsorption isotherms were measured at 77 K using a Quantachrome AS-1MP volumetric adsorption analyser. Before the adsorption measurements, all samples were outgassed for 24 h at 333 K in the degas port of the adsorption analyser.

Received 10 January 2003; accepted 23 April 2003; published 22 June 2003.

References

1. Muthukumar, M., Ober, C. K. & Thomas, E. L. Competing interactions and levels of ordering in self-organizing polymeric materials. *Science* **277,** 1225–1232 (1997).
2. Langley, P. J. & Hulliger, J. Nanoporous and mesoporous organic structures: new openings for materials research. *Chem. Soc. Rev.* **28,** 279–291 (1999).
3. Wulff, G. Molecular imprinting in crosslinked materials with the aid of molecular templates-a way towards artificial antibodies. *Angew. Chem. Int. Edn Engl.* **34,** 1812–1832 (1995).
4. Buchmeiser, M. R. New ways to porous monolithic materials with uniform pore size distribution. *Angew. Chem. Int. Edn Engl.* **40,** 3795–3797 (2001).
5. Peters, E. C., Svec, F. & Fréchet, J. M. J. Rigid macroporous polymer monoliths. *Adv. Mater.* **11,** 1169–1181 (1999).
6. Widawski, G., Rawiso, M. & François, B. Self-organized honeycomb morphology of star-polymer polystyrene films. *Nature* **369,** 387–389 (1994).
7. Chen, Y. Y., Ford, W. T., Materer, N. F. & Teeters, D. Facile conversion of colloidal crystals to ordered porous polymer nets. *J. Am. Chem. Soc.* **122,** 10472–10473 (2000).
8. Smith, R. C., Fischer, W. M. & Gin, D. L. Ordered poly(p-phenylenevinylene) matrix nanocomposites via lyotropic liquid-crystalline monomers. *J. Am. Chem. Soc.* **119,** 4092–4093 (1997).
9. Pindzola, B. A., Hoag, B. P. & Gin, D. L. Polymerization of a phosphonium diene amphiphile in the regular hexagonal phase with retention of mesostructure. *J. Am. Chem. Soc.* **123,** 4617–4618 (2001).
10. Zalusky, A. S., Olayo-Valles, R., Taylor, C. J. & Hillmyer, M. A. Mesoporous polystyrene monoliths. *J. Am. Chem. Soc.* **123,** 1519–1520 (2001).
11. Zalusky, A. S., Olayo-Valles, R., Wolf, J. H. & Hillmyer, M. A. Ordered nanoporous polymers from polystyrene-polylactide block copolymers. *J. Am. Chem. Soc.* **124,** 12761–12773 (2002).
12. Antonietti, M., Caruso, R. A., Göltner, C. G. & Weissenberger, M. C. Morphology variation of porous polymer gels by polymerization in lyotropic surfactant phases. *Macromolecules* **32,** 1383–1389 (1999).
13. Lee, H. K. *et al.* Synthesis of a nanoporous polymer with hexagonal channels from supramolecular discotic liquid crystals. *Angew. Chem. Int. Edn Engl.* **40,** 2669–2671 (2001).
14. Johnson, S. A., Ollivier, P. J. & Mallouk, T. E. Ordered mesoporous polymers of tunable pore size from colloidal silica templates. *Science* **283,** 963–965 (1999).
15. Liu, L., Li, P. S. & Asher, S. A. Entropic trapping of macromolecules by mesoscopic periodic voids in a polymer hydrogel. *Nature* **397,** 141–144 (1999).
16. Göltner, C. G. & Weissenberger, M. C. Mesoporous organic polymers obtained by 'twostep nanocasting' *Acta Polym.* **49,** 704–709 (1998).
17. Kim, J. Y., Yoon, S. B., Kooli, F. & Yu, J. S. Synthesis of highly ordered mesoporous polymer networks. *J. Mater. Chem.* **11,** 2912–2914 (2001).
18. Corma, A. From microporous to mesoporous molecular sieve materials and their use in catalysis. *Chem. Rev.* **97,** 2373–2419 (1997).
19. Ying, J. Y., Mehnert, C. P. & Wong, M. S. Synthesis and applications of supramolecular-templated mesoporous materials. *Angew. Chem. Int. Edn Engl.* **38,** 56–77 (1999).
20. Barton, T. J. *et al.* Tailored porous materials. *Chem. Mater.* **11,** 2633–2656 (1999).
21. Ryoo, R., Joo, S. H. & Jun, S. Synthesis of highly ordered carbon molecular sieves via template-mediated structural transformation. *J. Phys. Chem. B* **103,** 7743–7746 (1999).
22. Jun, S. *et al.* Synthesis of new, nanoporous carbon with hexagonally ordered mesostructure. *J. Am. Chem. Soc.* **122,** 10712–10713 (2000).
23. Ryoo, R., Joo S. H., Kruk, M. & Jaroniec, M. Ordered mesoporous carbons. *Adv. Mater.* **13,** 677–681 (2001).
24. Joo, S. H. *et al.* Ordered nanoporous arrays of carbon supporting high dispersions of platinum nanoparticles. *Nature* **412,** 169–172 (2001).
25. Lee, J. S., Joo, S. H. & Ryoo, R. Synthesis of mesoporous silicas of controlled pore wall thickness and their replication to ordered nanoporous carbons with various pore diameters. *J. Am. Chem. Soc.* **124,** 1156–1157 (2002).
26. Ramsay, J. D. F, Kallus, S. & Hoinkis, E. SANS characterisation of mesoporous silicas having model structures. *Stud. Surf. Sci. Catal.* **128,** 439–448 (2000).
27. Smarsly, B., Goltner, C. G., Antonietti, M., Ruland, W. & Hoinkis, E. SANS investigation of nitrogen sorption in porous silica. *J. Phys. Chem. B* **105,** 831–840 (2001).
28. Wang, J., Musameh, M. & Lin, Y. Solubilization of carbon nanotubes by nafion towards the preparation of amperometric biosensors. *J. Am. Chem. Soc.* **125,** 2408–2409 (2003).
29. Park, J. K. *et al.* In vivo nitric oxide sensor using non-conducting polymer-modified carbon fiber. *Biosens. Bioelectron.* **13,** 1187–1195 (1998).
30. Smits, F. M. Measurement of sheet resistivities with the four-point probe. *Bell System Tech. J.* 711 (May, 1958).

Acknowledgements

This work was supported in part by the Creative Research Initiative Program of the Korean Ministry of Science and Technology, and by the School of Molecular Science through Brain Korea 21 project. R.R. thanks O. Terasaki at Stockholm university for TEM measurements and helpful discussions.
Correspondence and requests for materials should be addressed to R.R.
Supplementary Information accompanies the paper on www.nature.com/naturematerials

Competing financial interests

The authors declare that they have no competing financial interests.

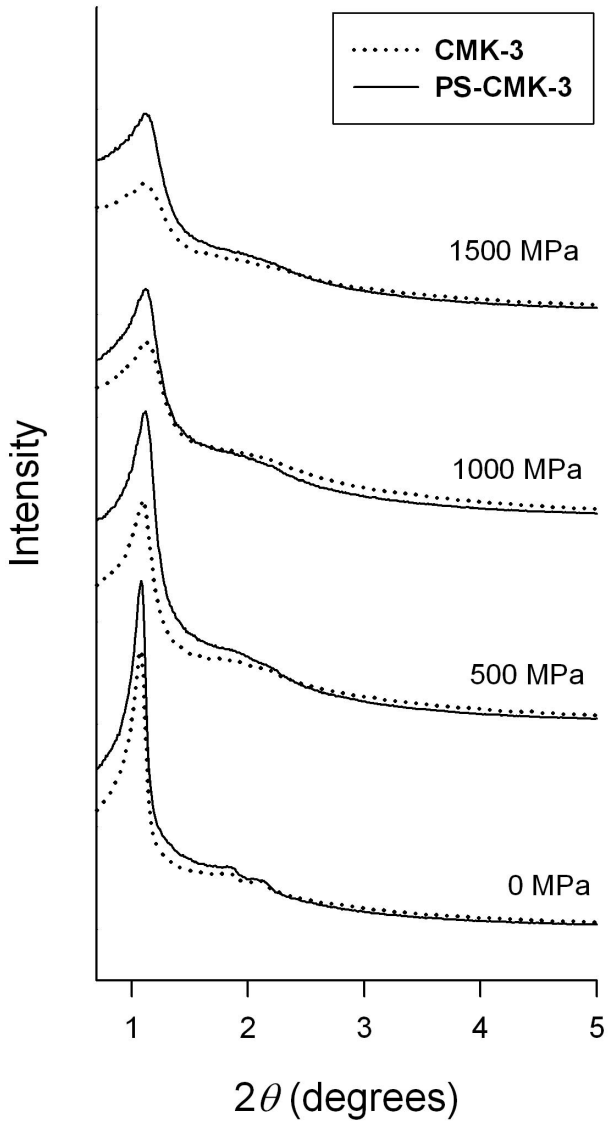

FIGURE S1

X-ray powder diffraction patterns of mesoporous carbon (CMK-3) and its composite with cross-linked polystyrene (PS-CMK-3), measured with a Rigaku Multiflex instrument (operated at 2.0 kW) after being compressed for 10 min at various pressures. The CMK-3 carbon exhibits high mechanical stability under compression despite highly porous structure. The mechanical stability increases further with the loading of 45wt% polymer, showing a synergistic enhancement between carbon framework and polymer layer.